Supplementary materials

The influence of nanomaterials on pyocyanin production by *Pseudomonas aeruginosa*

Joanna Jabłońska[1], Kamila Dubrowska[1], Adrian Augustyniak[1,2†], Rafał J. Wróbel[3], Mateusz Piz[4], Krzysztof Cendrowski[5], Rafał Rakoczy[1]

[1] West Pomeranian University of Technology in Szczecin, Faculty of Chemical Technology and Engineering, Department of Chemical and Process Engineering, Piastów avenue 42, 71-065 Szczecin, Poland

[2] Technische Universität Berlin, Chair of Building Materials and Construction Chemistry, Gustav-Meyer-Allee 25, 13355 Berlin, Germany

[3] West Pomeranian University of Technology in Szczecin; Faculty of Chemical Technology and Engineering; Department of Catalytic and Sorbent Materials Engineering; Pułaskiego 10, Szczecin, 70-322, Poland

[4] West Pomeranian University of Technology in Szczecin, Faculty of Chemical Technology and Engineering, Department of Inorganic Chemistry, Piastów avenue 42, 71-065 Szczecin, Poland

[5] West Pomeranian University of Technology in Szczecin; Faculty of Civil and Environmental Engineering; Department of General Civil Engineering; Piastów Avenue 50a, 70-311 Szczecin, Poland

Submitted to special issue NANO-2021 within the 9th International Conference "Nanotechnologies and Nanomaterials" NANO-2021

Materials and methods

XRD analysis

Powder Diffraction pattern of the commercial MWCNT (Sigma Aldrich) was recorded using the Empyrean II diffractometer (PANalytical, Netherlands) equipped with PIXcel3D detector. Copper tube ($\lambda 1,2 = 0.15418 \cdot 10^{-10}$ m) supplied with the voltage of 40 kV with the simultaneous intensity of the glow current at 35 mA, with bent graphite monochromator was used as a source of radiation and divergence slit 0.5º. The data were collected from 10º to 80º (2Θ), using the step size of 0.013º and the counting time of 0.3 s per step. Identification of phases, present in the sample, was performed on the basis of their X-ray characteristics contained in the PDF cards (PDF- 4+ 2021 ICDD database of powder diffraction patterns).

SEM-EDS analysis

Scanning electron microscopy with cold field emission (UHR FE-SEM Hitachi SU8020) was used to observe the morphology of the analyzed samples. Energy-dispersive X-ray spectroscopy (EDS) analysis was employed to determine elemental composition of MWCNT.

The biological samples were covered with metallic chromium coatings prior to measurements in order to avoid the charging effects. The 5 kV voltage was used during images acquisition. The metallic coatings were obtained by a magnetron sputtering method with the use of magnetron coater (Q150T; Quorum Technologies) equipped with a turbomolecular pump. The thickness of the conductive films was monitored with the use of quartz balance, which enables 0.1 nm measurement resolution.

Results

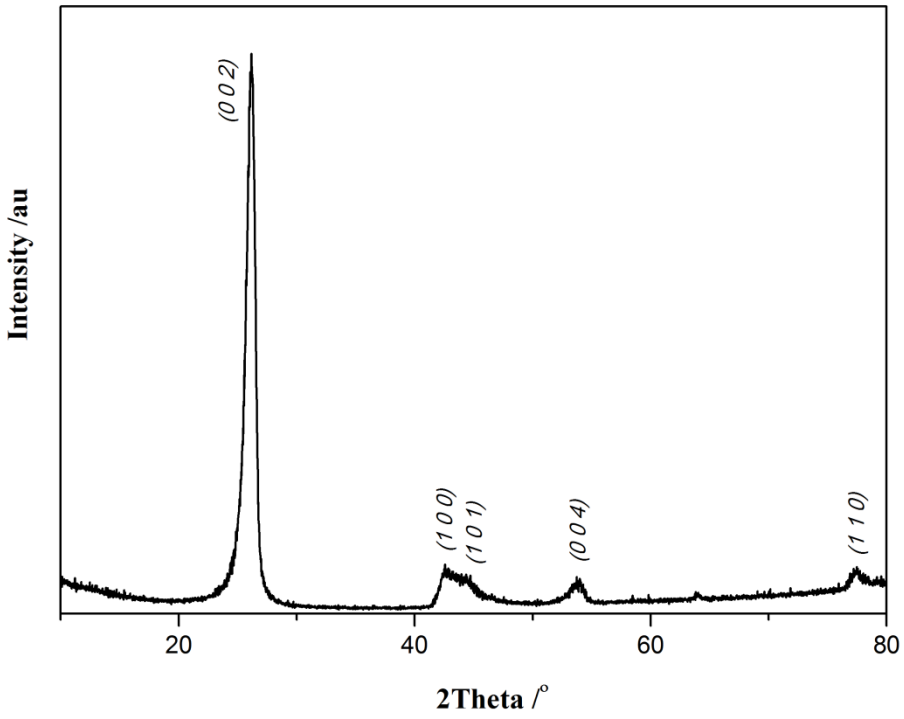

Fig.S1. XRD analysis of CNTs

Fig. S1 shows a fragment of the diffractogram of commercial carbon nanotubes (MWCNT) which is registered in the angular range 2Θ from 10 to 80°. Within this range, for 2θ equal to 26.16°, 42.47°, 44.73°, 53.79° and 77.41°, clear peaks were recorded in the diffraction pattern. The X-ray phase analysis showed that these peaks are consistent with the PDF 4+ card No: 00-041-1487, i.e. they

belong to the set characterizing carbon nanotubes. The material was identified by comparing the observed XRD peaks with the diffraction pattern of carbon nanotubes at the International Center for Diffraction Data (ICDD), which contains information on the location of the lines diffraction patterns and their relative intensity. Based on the results of X-ray qualitative phase analysis, it was confirmed that the commercial product contains carbon nanotubes (crystal system: hexagonal, a = 2.4704 Å, c = 6,7244 Å, space group *P63/mmc*), without a metal catalyst, which confirms their high degree of purity. The peaks recorded on the diffractogram correspond to reflections from planes (002), (100), (101), (004), (110), as shown in Fig. S1.

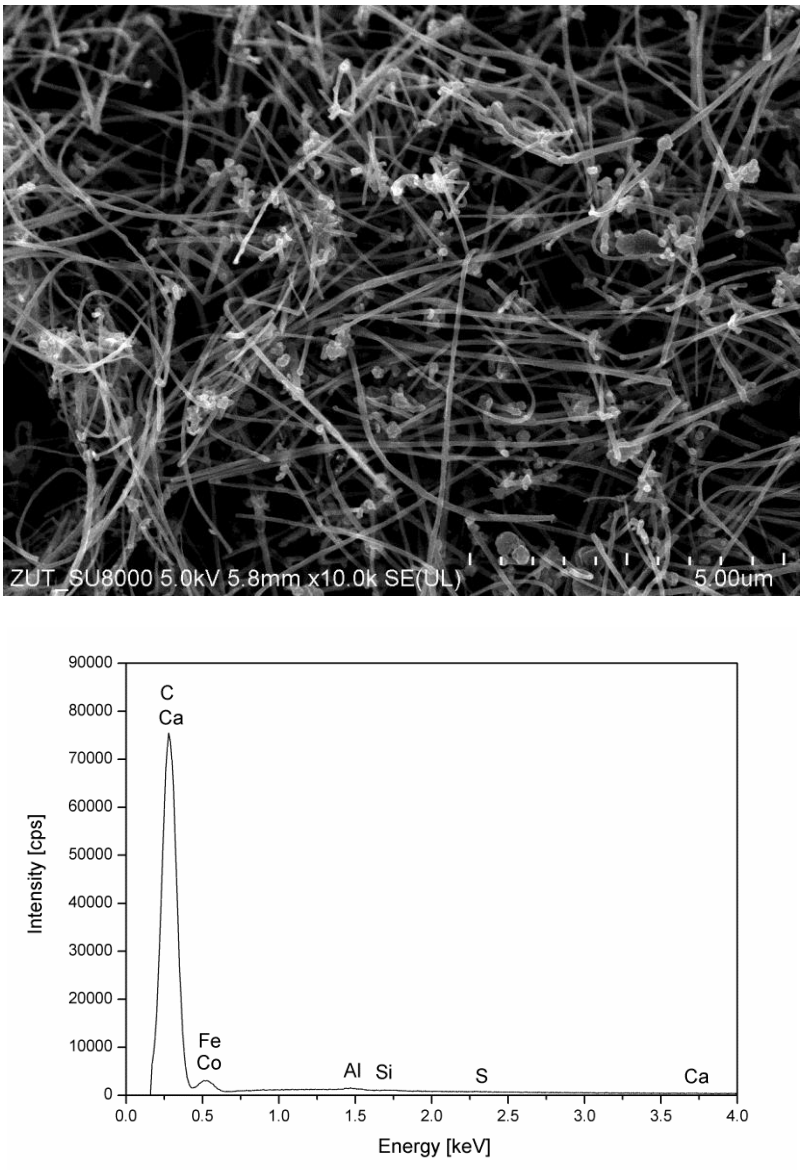

Fig. S2. SEM micrograph and EDS analysis of CNTs

SEM analysis of CNTs showed that their average width equaled 78.35 nm and was within the range declared by the producer (50-90 nm). Moreover, some aggregates of shapeless substance were noted and identified perhaps as amorphous carbon or catalyst that are a residue of the CVD synthesis method. Therefore, an additional analysis employing energy dispersive spectroscopy (EDS) was carried out. Elemental analysis showed high peak identified as carbon signal and smaller peaks assigned as iron, aluminum and silicon. Perhaps, they can be identified as catalyst (Fe) and catalyst carrier (Al, Si) that were not fully removed after synthesis. Moreover, some Ca, Co and S signals were noted. Nevertheless, these signals were residual.

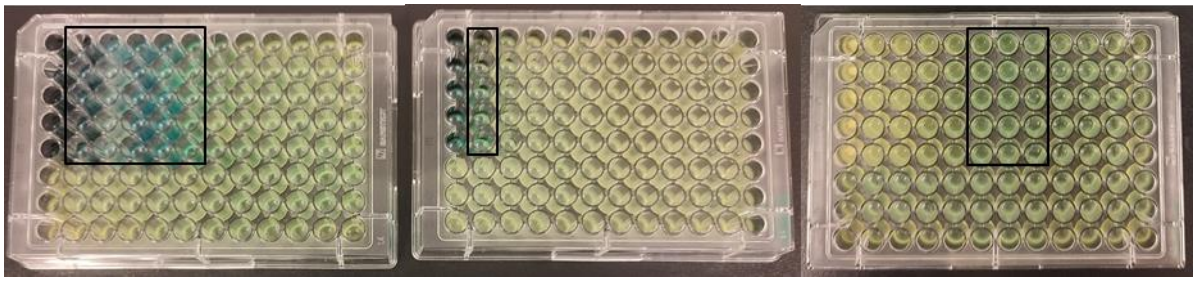

Fig. S3. Exemplary results showing the colours of *P. aeruginosa* cultures incubated with different concentrations of (from left to right): CNT-AA, CNT and ZnO nanoparticles

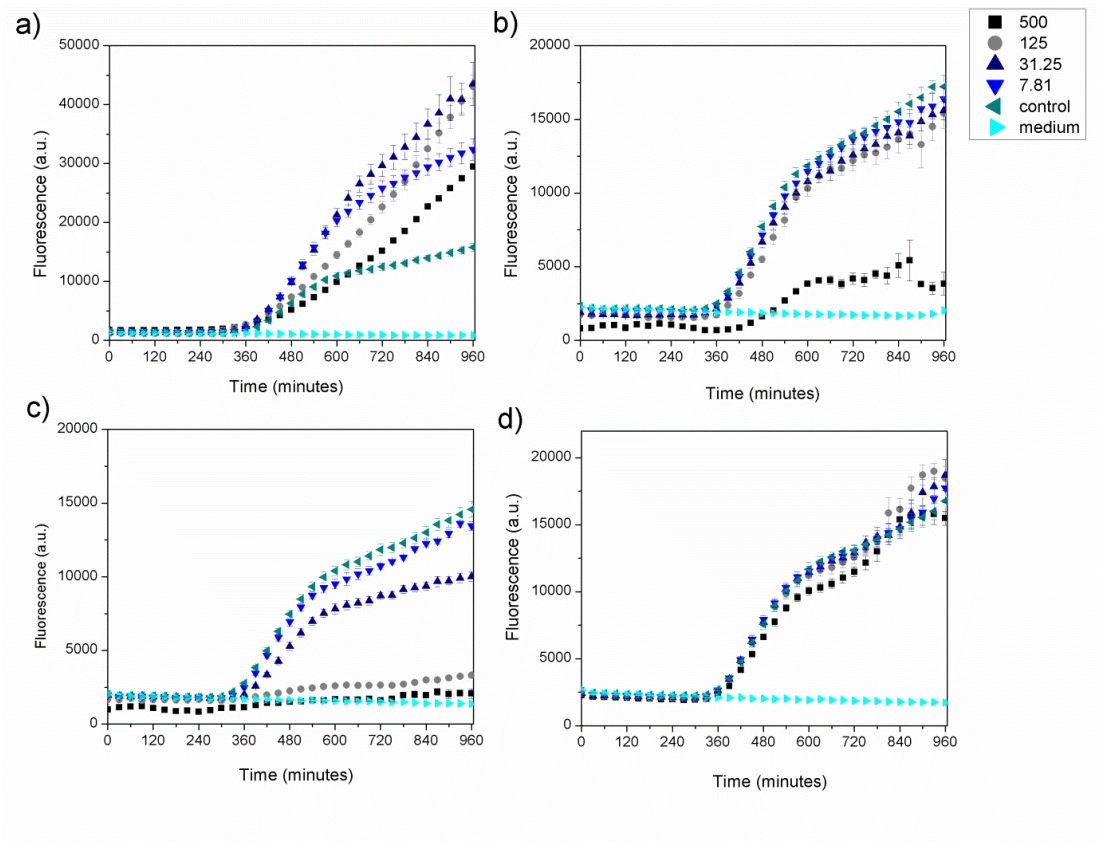

Fig. S4 The influence of different nanomaterial concentrations on general fluorescence of the culture a) ZnO, b) MWCNT and c) MWCNT with AA d) AA. Error bars indicate SEM (standard error of the mean)

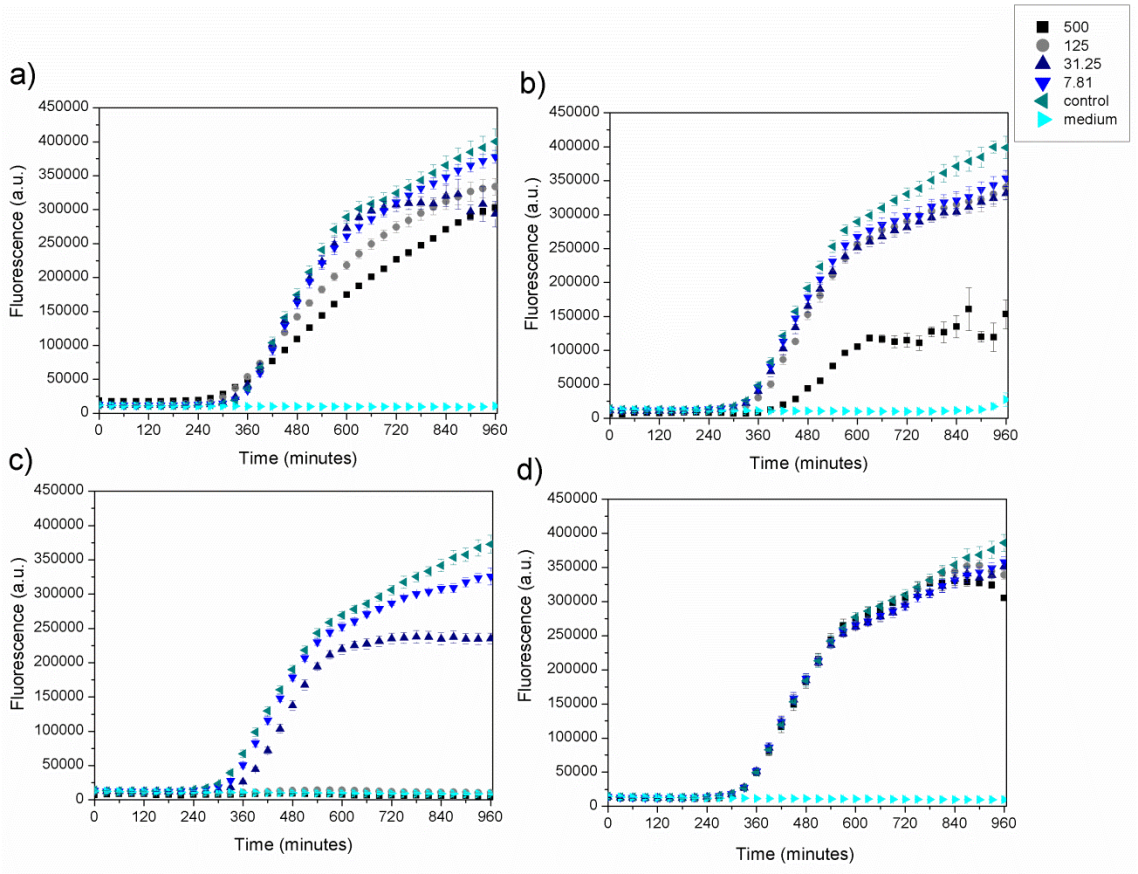

Fig. S5 The influence of different nanomaterial concentrations on pyoverdine production a) ZnO, b) MWCNT and c) MWCNT with AA d) AA. Error bars indicate SEM (standard error of the mean)

Tab. S1. ANOVA results of the analysis comparing different process conditions (E – conical (Erlenmeyer) flask, F – Falcon-type tube, PD – Petri dish, A – agitation 100 rpm, NA – no agitation, 10-50 – culture volume). '1' indicates a statistically significant difference at $p<0.05$

	E10NA	E20NA	E30NA	E40NA	E50NA	E10A	E20A	E30A	E40A	E50A	F10NA	F20NA	F30NA	F40NA	F50NA	F10A	F20A	F30A	F40A	F50A	PD
E10NA																					
E20NA	0																				
E30NA	1	0																			
E40NA	1	1	0																		
E50NA	1	1	0	0																	
E10A	1	0	0	0	0																
E20A	1	0	0	0	0	0															
E30A	1	1	0	0	0	0	0														
E40A	1	1	0	0	0	0	0	0													
E50A	1	1	0	0	0	0	0	0	0												
F10NA	1	0	0	0	0	0	0	0	0	0											
F20NA	1	1	0	0	0	0	0	0	0	0	0										

F30NA	1	1	0	0	0	0	0	0	0	0	0	0									
F40NA	1	1	0	0	0	0	0	0	0	0	0	0	0								
F50NA	1	1	0	0	0	0	0	0	0	0	0	0	0	0							
F10A	1	0	0	0	0	0	0	0	0	0	0	0	0	0	0						
F20A	1	1	0	0	0	0	0	0	0	0	0	0	0	0	0	0					
F30A	1	1	0	0	0	0	0	0	0	0	0	0	0	0	0	0	0				
F40A	1	1	0	0	0	0	0	0	0	0	0	0	0	0	0	0	0	0			
F50A	1	1	0	0	0	0	0	0	0	0	0	0	0	0	0	0	0	0	0		
PD	1	1	1	1	1	1	1	1	1	1	1	1	1	1	1	1	1	1	1	1	